# Kinetics of the NCN Radical

**Randall E. Baren and John F. Hershberger***

*Department of Chemistry, North Dakota State University, Fargo, North Dakota 58105*

*Received: April 3, 2002; In Final Form: August 12, 2002*

The kinetics of the NCN + NO reaction has been studied using laser-induced fluorescence spectroscopy over the temperature range 298−573 K to measure total rate constants and time-resolved infrared diode laser spectroscopy as a probe for possible products. The reaction has a rate constant of $k(\mathrm{NCN} + \mathrm{NO}) = (2.88 \pm 0.2) \times 10^{-13}$ cm$^3$ molecule$^{-1}$ s$^{-1}$ at 298 K and low (~3 Torr) total pressure. The rate constant displays both a temperature as well as a pressure dependence, indicating that adduct formation is a major product channel. Only very small amounts of other products were detected. Upper limits for the low-pressure rate constants of NCN + $O_2$, $C_2H_4$, and $NO_2$ were also obtained.

## Introduction

Nitrogen oxides are of great interest because of their toxic effects as atmospheric pollutants generated from the combustion of fossil fuels. The mechanisms and rate parameters for reactions involving nitrogen compounds have been extensively investigated in order to understand combustion generated air pollution.[1]

One of several routes for the production of NO is the "prompt NO," or Fenimore mechanism.[2] This process has long been thought to principally involve the spin-forbidden reaction[1,3−10]

$$\mathrm{CH}(^2\Pi) + \mathrm{N_2} \rightarrow \mathrm{HCN} + \mathrm{N}(^4\mathrm{S}) \qquad (1)$$

followed by oxidation of HCN and N. Recently, the work by Lin et al.[11,12] has suggested an alternative spin-allowed product channel:

$$\mathrm{CH}(^2\Pi) + \mathrm{N_2} \rightarrow \mathrm{H} + \mathrm{NCN}(^3\Sigma_g^-) \qquad (2)$$

The chemistry of the cyanonitrene (NCN) diradical is therefore of interest in the modeling of hydrocarbon flames. This species has been the subject of several spectroscopic studies. In early work, Jennings and Linnett observed an emission at 329 nm upon the introduction of hydrocarbons and nitrogen into a flame.[13] Herzberg and Travis[14] monitored the UV absorption spectrum of NCN upon flash photolysis of diazomethane. Similar work by Kroto[15] and Jacox[16] used cyanogen azide as a photolytic precursor. Smith et al. proposed NCN as an intermediate in the combustion of nitramine propellant molecules.[17] Ultraviolet emission studies have also suggested that NCN is present, and is a source of CN radicals, in the comet Brorosen-Metcalf.[18] Additionally, NCN has been suggested as a critical growth species in the synthesis of carbon nitride ($C_3N_4$).[19] Surprisingly, there have been no reported measurements for the gas phase kinetics of reactions of NCN, although several early reports have appeared in organic chemistry literature on insertion reactions of nitrenes with hydrocarbons.[20−23]

This work reports the kinetic study of the reaction of NCN with NO. The NCN radical is produced by the 193 nm excimer laser photolysis of diazomethane in the presence of cyanogens ($C_2N_2$).

$$\mathrm{CH_2N_2} + \mathrm{C_2N_2} + h\nu\ (193\ \mathrm{nm}) \rightarrow \mathrm{NCN} + \text{other products} \qquad (3)$$

This method has been used previously for the production of NCN in early spectroscopic studies.[14,24] Laser-induced fluorescence near 329 nm via the well characterized $A^3\Pi_u \leftarrow X^3\Sigma_g^-$ transition[17,25,26] is used to measure the total rate constant of the NCN + NO reaction as a function of temperature and pressure. This reaction has several possible product channels:

$$\mathrm{NCN} + \mathrm{NO} \rightarrow \mathrm{N_2O} + \mathrm{CN} \qquad \Delta H_r^0 = -25.8\ \mathrm{kJ/mol} \qquad (4a)$$

$$\rightarrow \mathrm{N_2} + \mathrm{NCO} \qquad \Delta H_r^0 = -411.6\ \mathrm{kJ/mol} \qquad (4b)$$

$$\rightarrow \mathrm{N_2} + \mathrm{CNO} \qquad \Delta H_r^0 = -110.9\ \mathrm{kJ/mol} \qquad (4c)$$

$$\rightarrow \mathrm{CO} + \mathrm{N_3} \qquad \Delta H_r^0 = -239.3\ \mathrm{kJ/mol} \qquad (4d)$$

$$\rightarrow \mathrm{CNN} + \mathrm{NO} \qquad \Delta H_r^0 = +126.4\ \mathrm{kJ/mol} \qquad (4e)$$

$$\rightarrow \mathrm{NCNNO} \qquad (4f)$$

Thermochemical information was taken from standard JANAF tables,[27] except for NCO, where a value of $\Delta H_f^0 = 131.38$ kJ/mol was used,[28] CNO, where a value of $\Delta H_f^0 = 432.19$ kJ/mol was used,[29,30] NCNNO adduct, for which thermochemical information is unknown, and for both NCN and CNN, for which $\Delta Hf^0 = 452.71$ and 579.06 kJ/mol were used, respectively.[31]

## Experimental Section

The experimental apparatus using an LIF technique for kinetics measurements has been described previously.[32] Only a brief description will be given here. The photolysis laser light was provided by an excimer laser (Lambda Physik COMPEX 200) operating at 193 or 248 nm and a repetition rate of 4 Hz. Typical photolysis pulse energies were 2−6 mJ. The 329.008 nm probe light (~0.5 mJ/pulse) was produced by frequency

10.1021/jp0208844 CCC: $22.00 
Published on Web 10/23/2002

doubling 658.016 nm light from a dye laser (Continuum ND-6000) pumped by the second harmonic of a Nd:YAG laser (Continuum Surelite II-10). The probe laser was operated at a repetition rate of 8 Hz. The photolysis and probe beams were made collinear using a dichroic mirror and copropagated down a Pyrex reaction cell. Fluorescence was detected 90° from the laser beams using an R508 photomultiplier tube. A 320 nm long-pass filter was used to eliminate the detection of photolysis light. Spectroscopic studies have indicated that most of the emission occurs at the 329 nm excitation wavelength, making it difficult to filter out scattered probe light.[17] Fortunately, the LIF emission is sufficiently strong that scattered probe light does not severely affect the signals. The unamplified PMT signal was recorded by a boxcar integrator (Stanford Instruments model 250) with a 10-60 ns delay and a 400 ns gate width then averaged on a personal computer. A digital delay generator (Stanford DG535) was used to vary the delay between excimer and dye laser pulses in order to produce an NCN concentration vs time profile. The static cell was resistively heated to collect data at elevated temperatures up to 573 K. Gases introduced into the reaction cell were allowed to mix for 10 min to ensure complete mixing and thermal equilibration.

The infrared absorption apparatus for product molecule detection of $N_2O$ and $CO_2$ has been described in previous publications.[33−35] 193 nm photolysis light was made collinear with probe light from a tunable lead-salt diode laser (Laser Photonics) and copropagated down a 1.46 m absorption cell. After removal of the UV light, the infrared beam passed through a 1/4 m monochromator and was focused onto a 1 mm InSb detector (Cincinnati Electronics, ∼1 $\mu$s response time). Transient infrared absorption signals were recorded on a digital oscilloscope (LeCroy 9310A) and transferred to a computer for analysis. $N_2O$ and $CO_2$ product yields were probed by using the following absorption lines:

$$CO_2\ ((00°0),J{=}12) \rightarrow CO_2\ ((00°1),J{=}13)$$

R(12) line at 2358.728 $cm^{-1}$

$$N_2O\ ((00°0),J{=}21) \rightarrow N_2O\ ((00°1)\ J{=}20)$$

P(21) line at 2204.715 $cm^{-1}$

The HITRAN molecular infrared database[36] was used to locate and identify the spectral absorption lines of $N_2O$ and $CO_2$. When detecting $CO_2$ as a product, the infrared laser beam path was purged with $N_2$ to remove atmospheric $CO_2$.

$SF_6$ (Matheson) was purified by repeated freeze−pump−thaw cycles at 77 K. NO (Matheson) was purified by vacuum distillation at 77 and 163 K. $NO_2$ (Matheson) was purified by vacuum distillation at 77 and 220 K. $O_2$ (Matheson) was used without further purification. $C_2H_4$ was purified by several freeze−pump−thaw cycles at 77 K. Cyanogen ($C_2N_2$) was synthesized by the reaction of copper sulfate with aqueous sodium cyanide[37] and purified by freeze−pump−thaw cycles at 77 K as well as vacuum distillation at 223 K to remove $CO_2$. Diazomethane ($CH_2N_2$) was synthesized by the reaction of MNNG (1-methyl-3-nitro-1-nitrosoguanidine, $C_2H_5N_5O_3$) with aqueous sodium hydroxide[38] and purified by vacuum distillation at 223 K to remove air and $CO_2$. Traces of $CO_2$ were removed from $SF_6$, $C_2N_2$ and $CH_2N_2$ by the use of an ascarite trap.

Typical reaction conditions for the LIF experiments were $P_{CH_2N_2}$ = 0.05−0.10 Torr, $P_{C_2N_2}$ = 0.20 Torr, $P_{NO}$ = 0−6.0 Torr (NCN + NO), $P_{C_2H_4}$ 0−0.60 Torr (NCN + $C_2H_4$), $P_{NO_2}$ = 0−2.0 Torr (NCN + $NO_2$), $P_{O_2}$ = 0−5.0 Torr (NCN + $O_2$), and $P_{He}$ = 0−600 Torr (NCN + NO). Pressure dependent studies, for the reaction of NCN + NO, used He as an inert gas to collect kinetic data from 50 to 600 Torr total pressure. LIF experiments were conducted under pseudofirst-order conditions with [NO], [$C_2H_4$], [$NO_2$] or [$O_2$] ≫ [NCN]. Typical conditions for the infrared experiments were $P_{CH_2N_2}$ = 0.10 Torr, $P_{C_2N_2}$ = 0.20 Torr, $P_{SF_6}$ = 1.0 Torr, and $P_{NO}$ = 0−1.0 Torr.

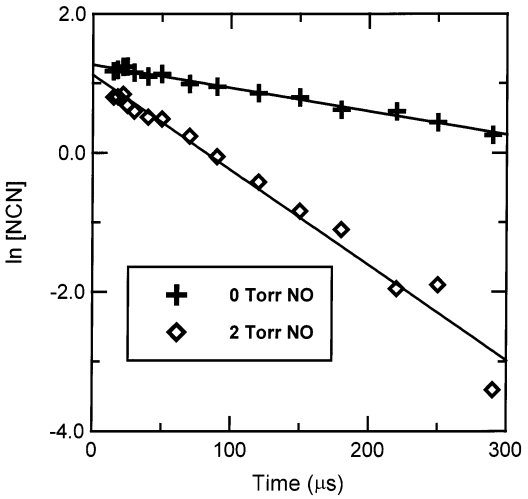


**Figure 1.** NCN laser-induced fluorescence signals as a function of time. Reaction conditions: $P_{CH_2N_2}$ = 0.05 Torr, $P_{C_2N_2}$= 0.2 Torr. 193 nm photolysis.

## Results

Previous spectroscopic studies have identified several bands in the LIF spectrum of the $A^3\Pi_u \leftarrow X^3\Sigma_g^-$ transition of NCN.[17] We choose the (0−0) band at 329.008 nm for NCN detection. The following control experiments were performed to ensure that the fluorescence signals were indeed from NCN alone: The 193 nm photolysis of diazomethane alone produced very little LIF signal. This is consistent with previous reports that this precursor alone produces only small amounts of NCN.[14] Photolysis of $C_2N_2$ alone produced no signal, indicating the CN radicals are not detected at the probe wavelength used. Upon 193 nm photolysis of $CH_2N_2/C_2N_2$ mixtures, large LIF signals with ∼200 ns lifetimes were observed at 329.008 nm. When the dye laser was detuned off of this spectral line, no LIF signal was observed.

**NCN + NO Reaction.** Figure 1 shows typical boxcar integrated signal amplitudes as a function of pump−probe delay time between excimer and dye laser pulses. The NCN signals displayed rise times on the order of ∼15 $\mu$s followed by slower decay times of ∼200 $\mu$s. The rise is attributed to formation of NCN through photolysis and subsequent reaction of $CH_2N_2/C_2N_2$ mixtures. It is possible that NCN is formed vibrationally excited. $SF_6$ is known to be an efficient relaxer of vibrational excitation of several triatomic molecules.[39,40] The rise and decay rates of the LIF signals were not affected by the addition of $SF_6$ buffer gas; however, the signal magnitudes were noticeably smaller, presumably due to fluorescence quenching effects. The unchanged temporal response suggests that NCN is either produced vibrationally cold or vibrational relaxation occurs within ∼15 $\mu$s even in the absence of buffer gas. Most of the LIF experiments reported here were performed without $SF_6$ buffer gas.

When nitric oxide was added to the reaction mixture, an increase in the NCN decay rate was observed. In the presence of added reactant, pseudo-first-order conditions apply and a

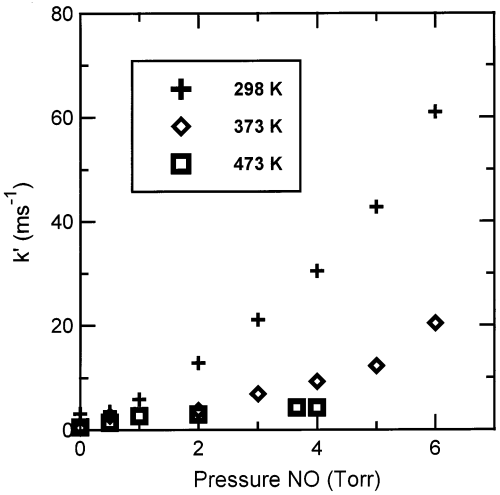


**Figure 2.** Pseudofirst-order decay rates of NCN LIF signals as a function of NO pressure. $CH_2N_2$ and $C_2N_2$ pressures are the same as those in Figure 1.

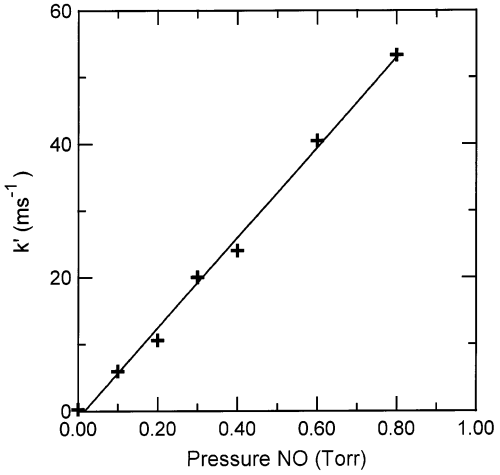


**Figure 3.** Pseudofirst-order decay rates of NCN LIF signals as a function of NO pressure, in the presence of added He buffer gas. Reaction conditions: $P_{CH_2N_2} = 0.05$ Torr, $P_{C_2N_2} = 0.2$ Torr, $P_{NO} = 0.0-0.8$ Torr, $P_{He} = 100.0$ Torr, $T = 298$ K.

standard kinetic analysis results in

$$[NCN] = [NCN]_0 e^{(-k't)}$$

$$k' = k_4[NO] + k_D$$

where $k'$ is the observed pseudofirst-order rate constant, $k_4$ is the desired bimolecular rate constant for the NCN + NO reaction, and $k_D$ represents the decay rate in the absence of added nitric oxide. Contributions to $k_D$ include self-reaction, reaction with one or more precursor molecules, and diffusion of detected species out of the probed volume. Figure 2 shows the pseudo-first-order decays, $k'$, as a function of NO pressure at several different temperatures. In the absence of added NO, very small values of $k'$ were observed, indicating that the concentration of transient species was quite low, and that radical−radical chemistry other than the title reaction did not significantly affect the results. The slope of these plots represents the desired bimolecular rate constant $k_4$. As is apparent in Figure 2, the slope is not constant, indicating significant deviation from second order kinetics, especially in the 298 K data. This is attributed to a dependence of the bimolecular rate constant on total pressure (which is not held constant in the experiments

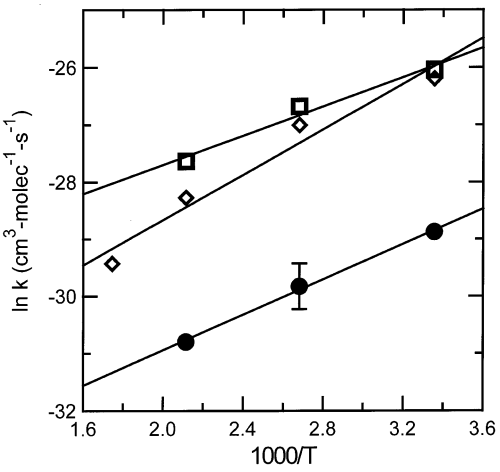


**Figure 4.** Arrhenius plot of the NCN + NO reaction at pressures of ~2 Torr (●), 300 Torr (◇), and 600 Torr (□) total pressure. $CH_2N_2$ and $C_2N_2$ pressures are the same as in Figures 1 and 2. $P_{He} = 0$, 300, and 600 Torr, respectively.

shown in Figure 2). Figure 3 shows a plot of $k'$ vs NO pressure when 100 Torr of He was included in the reaction mixture. This plot shows a much greater slope than in Figure 2, indicating a pressure dependence in $k_4$. Furthermore, the curvature seen in Figure 2 is not apparent in Figure 3, because the total pressure under the conditions of Figure 3 is very nearly constant, varying only from 200.05 to 200.85 Torr.

Kinetic experiments for the reaction of NCN + NO were conducted over the temperature range from 298 to 573 K. Figure 4 illustrates an Arrhenius plot for the measured rate constant, $k_4$, over the temperature range from 298 to 573 K with error bars representing one standard deviation. Experiments were also performed to examine the dependence of this reaction on total pressure. Figure 5 shows the NCN + NO rate constant measured at 298, 373, 473 and 573 K as a function of added He. The rate constants total pressures of ~3, 300, and 600 Torr (in cm$^3$ molecule$^{-1}$ s$^{-1}$, 1 $\sigma$ error bars), respectively, are represented by

$$k_4 = (1.706 \pm 0.39) \times 10^{-15} e^{[(1545.2\pm85.4)/T]} \quad (\sim 3 \text{ Torr})$$

$$k_4 = (8.605 \pm 5.33) \times 10^{-15} e^{[(1983.2\pm284.5)/T]} \quad (300 \text{ Torr})$$

$$k_4 = (8.663 \pm 4.56) \times 10^{-15} e^{[(1272.6\pm212.1)/T]} \quad (600 \text{ Torr})$$

The values of $k_4$ at 3 Torr were obtained by estimating the slope of the tangent of the curves in Figure 2 at $P_{NO} = 3.0$ Torr. When 100−600 Torr of helium was included in the reagent mixture, no curvature was observed in the plots of pseudofirst-order rate constant vs [NO], because under these conditions the total pressure was essentially constant. Least squares best fit lines of the $k'$ vs [NO] data were therefore used to determine $k_4$.

Product detection in reaction 4 was measured at 298 K using infrared absorption spectroscopy. Very small amounts of $N_2O$ and $CO_2$ molecules were detected, as shown in the transient absorption signals of Figure 6. The $CO_2$ signal is noisy, partly because of the presence of a small amount of static $CO_2$ impurity in the $CH_2N_2$ samples (frequency jitter in the infrared laser causes larger amplitude noise in the signal when a significant static absorption line is present). The rise times observed are consistent with production of products in excited vibrational states, followed by relaxation into the ground vibrational state in the presence of $SF_6$ buffer gas.[40,41] Absorption signals were

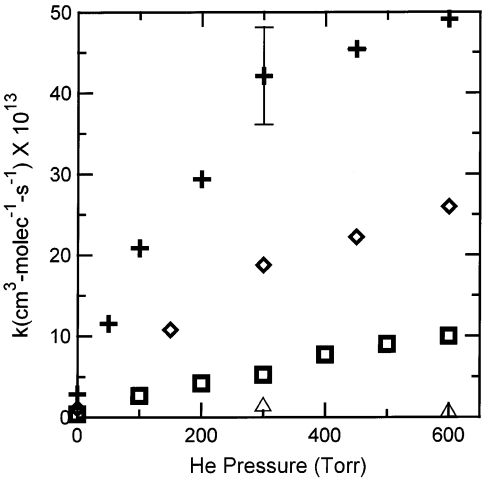


**Figure 5.** Pressure dependence of the NCN + NO bimolecular rate constant at temperatures of 298 K (+), 373 K (◇), 473 K (□), and 573 K (△).

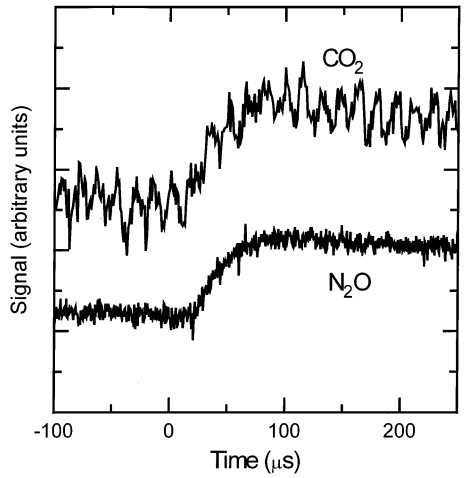


**Figure 6.** Transient infrared absorption signals for $N_2O$ and $CO_2$ product molecules. Lines probed: $N_2O$ (00°1) ← (00°0) P(21) at 2204.715 $cm^{-1}$ and $CO_2$ (00°1) ← (00°0) R(12) at 2358.728 $cm^{-1}$. Each transient was obtained from a single photolysis laser shot. Reaction conditions: $P_{CH_2N_2} = 0.10$ Torr, $P_{C_2N_2} = 0.20$ Torr, $P_{SF_6} = 1.0$ Torr, and $P_{NO} = 0.20$ Torr.

converted to number densities using tabulated line strengths and equations described previously.[33] Typical number densities of $[N_2O] \approx 3 \times 10^{11}$ and $[CO_2] \approx 1.6 \times 10^{11}$ molecule $cm^3$ were obtained for the signals in Figure 6. These concentrations are 1−2 orders of magnitude smaller than typical values obtained in similar experiments,[42,43] suggesting that the pathways leading to these products are of only minor importance, although our lack of information regarding initial NCN concentrations prevents a quantitative comparison.

This system is complicated by several possible secondary reactions. If NCO is produced in channel 4b, both $N_2O$ and $CO_2$ would be formed by the reaction

$$NCO + NO \rightarrow N_2O + CO \quad (5a)$$

$$\rightarrow CO_2 + N_2 \quad (5b)$$

Since the branching ratios of reaction 5 are known ($\phi_{5a} = 0.44$ and $\phi_{5b} = 0.56$ at 298 K),[33] it is possible in principle to estimate the amount of $N_2O$ produced in channel 5a if it is assumed that channel 5b is the only source of $CO_2$. Any excess $N_2O$ would then be attributed to channel 4a (note that CN produced in channel 4a would not quickly react with NO at low pressures). Unfortunately, other complications make the reliability of this approach questionable. For example, $^1CH_2$ formed in the $CH_2N_2$ photolysis could react with NO, possibly forming NCO as well. The products of $^1CH_2$ + NO are not well characterized. Furthermore, product channels such as 4c, $N_2$ + CNO, or 4d, CO + $N_3$, could also result in secondary chemistry. $N_3$ + NO presumably produces $N_2 + N_2O$, and the products of the CNO + NO reaction are not quantitatively known. In general, our results suggest that both channels 4a and 4b are active to some minor extent, but a quantitative determination of the branching ratio will require further experiments, probably involving different precursors for NCN formation. The observation of significant pressure dependence in the total rate constants suggests that adduct formation, channel 4f, is a major and possibly dominant product channel. No attempts were made to detect NCNNO, for which no spectroscopic information is known.

**NCN + $C_2H_4$, $O_2$, $NO_2$ Reactions.** Reactions of NCN with $C_2H_4$, $O_2$, and $NO_2$ were also investigated. There was no significant increase in NCN pseudofirst-order decay rates upon addition of several Torr of these molecules. This indicates that these reactions are extremely slow, at least at low total pressures. Estimated upper limits for the rate constants of reaction of NCN at 298 K in the 1−3 Torr pressure range are: $k(NCN + C_2H_4) < 8.5 \times 10^{-15}$ $cm^3$ $molecule^{-1}$ $s^{-1}$, $k(NCN + O_2) < 1.0 \times 10^{-14}$ $cm^3$ $molecule^{-1}$ $s^{-1}$, and $k(NCN + NO_2) < 1.5 \times 10^{-14}$ $cm^3$ $molecule^{-1}$ $s^{-1}$.

## Discussion

This study represents the first report of direct measurements of the kinetics of the NCN radical. We are aware of only one previous report of any kinetic information on this species. In a recent modeling study of NO-reburning processes, several NCN reactions were included with estimated rate parameters, including the estimate of $k = 1.6 \times 10^{-11}$ $cm^3$ $molecule^{-1}$ $s^{-1}$ for the NCN + $O_2$ reaction.[44] This value is several orders of magnitude greater than our estimate of an upper limit for the rate constant. Although it is possible that this reaction is faster at higher pressures and/or temperatures, it is still likely that this rate constant was overestimated in the modeling study. Further work on the temperature and pressure dependence of the NCN + $O_2$ reaction is necessary.

The mechanism responsible for the formation of NCN is not well understood at this time. At least two routes are possible:

$$CH_2N_2 + h\nu\ (193\ nm) \rightarrow {}^1CH_2 + N_2 \quad (6a)$$

$${}^1CH_2 + C_2N_2 \rightarrow NCN + C_2H_2 \quad (6b)$$

or

$$C_2N_2 + h\nu\ (193\ nm) \rightarrow 2CN \quad (7a)$$

$$CN + CH_2N_2 \rightarrow NCN + CH_2N \quad (7b)$$

If reaction 7 is a major route for NCN formation, then in principle CN radical precursors other than $C_2N_2$ should also work. For example, ICN photolysis at 248 nm produces CN radicals in high yields. We attempted to detect NCN produced from 248-nm photolysis of $ICN/CH_2N_2$ mixtures. No LIF signals were detected, suggesting that reaction 7b does not occur, and that reactions 6a and 6b (or some other, unknown, mechanism) are the dominant routes to NCN formation.

No high level ab initio calculations on the title reaction have been reported. Wang et al., however, reported an experimental and BAC-MP4 computational study of the reverse reaction[45]

$$CN + N_2O \rightarrow NCNNO \rightarrow NCN + NO \qquad (8)$$

They found $k_8$ to be immeasurably slow below 500 K, as expected for an endothermic process. The calculations predicted an NCNNO adduct that lies approximately 75 kJ/mol below NCN + NO, with only small barriers to reach the adduct from either NCN + NO or CN + $N_2O$. They did not calculate $k_4$, so no direct comparison can be made, but their prediction of a fairly deep NCNNO well is qualitatively consistent with our observations.

## Conclusions

The NCN + NO reaction proceeds primarily through adduct formation as evidenced by significant pressure dependence of the rate constant. At 298 K, this reaction has a rate constant of $(2.88 \pm 0.2) \times 10^{-13}$ cm$^3$ molecule$^{-1}$ s$^{-1}$ at a low total pressure of ~3 Torr, but the rate constant increased with pressure, reaching a high-pressure limit of $(5.0 \pm 0.5) \times 10^{-12}$ cm$^3$ molecule$^{-1}$ s$^{-1}$. The reaction displays a negative temperature dependence typical of radical−radical reactions. Only very small amounts of $N_2O$ products were detected. These results suggest that NCNNO adduct formation is the dominant product channel.

**Acknowledgment.** This work was supported by the Division of Chemical Sciences, Office of Basic Energy Sciences of the Department of Energy, Grant DE-FG03-96ER14645.

## References and Notes

(1) Miller, J. A.; Bowman, C. T. *Prog. Energy Combust. Sci.* **1989**, *15*, 287.
(2) Fenimore, C. P. *Int. Symp. Combust.* **1971**, *13*, 373.
(3) Cui, Q.; Morokuma, K. *Theor. Chem. Acta* **1999**, *102*, 127.
(4) Fulle, D.; Hippler, H. *J. Chem. Phys.* **1996**, *105*, 5423.
(5) Berman, M. R.; Lin, M. C. *J. Phys. Chem.* **1983**, *87*, 3933.
(6) Medhurst, L. J.; Garland, N. J.; Nelson, H. H. *J. Phys. Chem.* **1993**, *97*, 12275.
(7) Becker, K. H.; Engelhardt, B.; Geiger, H.; Kurtenbach, R.; Schrey, G.; Wiesen, P. *Chem. Phys. Lett.* **1992**, *195*, 322.
(8) Rodgers, A. S.; Smith, G. P. *Chem. Phys. Lett.* **1996**, *253*, 313.
(9) Miller, J. A. *Int. Symp. Combustion* **1996**, *26*, 461.
(10) Miller, J. A.; Bowman, C. T. *Int. J. Chem. Kinet.* **1991**, *23*, 289.
(11) Moskaleva, L. V.; Lin, M. C. *J. Phys. Chem. A* **2001**, *105*, 4156.
(12) Lin, M. C.; Moskaleva, L. V.; Xia, W. S. *Chem. Phys. Lett.* **2000**, *331*, 269.
(13) Jennings, K. R.; Linnett, J. R. *Trans. Faraday Soc.* **1960**, *56*, 1737.
(14) Herzberg, G.; Travis, D. N. *Can. J. Phys.* **1964**, *42*, 1658.
(15) Kroto, H. W. *Can. J. Phys.* **1967**, *45*, 1439.
(16) Milligan, D. E.; Jacox, M. E. *J. Chem. Phys.* **1966**, *45*, 1387.
(17) Smith, G. P.; Copeland, R. A.; Crosley, D. R. *J. Chem. Phys.* **1989**, *91*, 1987.
(18) O'dell, C. R.; Miller, C. O.; Cochran, A. L.; Cochran, W. D.; Opal, C. B.; Barker, E. S. *Astrophys. J.* **1991**, *368*, 616.
(19) Benard, D. J.; Linnen, C.; Harker, A. *J. Phys. Chem. B* **1998**, *102*, 6010.
(20) Barton, D. H. R.; Morgan, L. R. *J. Chem. Soc.* **1962**, 622.
(21) Barton, D. H. R.; Starratt, A. N. *J. Chem. Soc.* **1965**, 2444.
(22) Lwowski, W.; Mattingly, T. W. *Tetrahedron Lett.* **1962**, 277.
(23) Anastassiou, A. G.; Simmons, H. E. *J. Am. Chem. Soc.* **1967**, *89*, 3177.
(24) Herzberg, G. *Proc. R. Soc. A* **1961**, *262*, 291.
(25) Beaton, S. A.; Ito, Y.; Brown, J. M. *J. Mol. Spectrosc.* **1996**, *178*, 99.
(26) Beaton, S. A.; Brown, J. M. *J. Mol. Spectrosc.* **1997**, *183*, 347.
(27) Chase, M. S. J. *J. Phys. Chem. Ref. Data*, **1985**, *14*, 1.
(28) East, A. L. L.; Allen, W. D. *J. Chem. Phys.* **1993**, *99*, 4638.
(29) Grussdorf, J.; Temps, F.; Wagner, H. Gg. *Ber. Bunsen-Ges. Phys. Chem.* **1997**, *101*, 134.
(30) Su, H.; Kong, F. *J. Chem. Phys.* **2000**, *113*, 1885.
(31) Clifford, E. P.; Wenthold, P. G.; Lineberger, W. C.; Petersson, G. A.; Broadus, K. M.; Kass, S. R.; Kato, S.; DePuy, C. H.; Bierbaum, V. M.; Ellison, G. B. *J. Phys. Chem. A* **1998**, *102*, 7100.
(32) Baren, R. E.; Hershberger, J. F. *J. Phys. Chem. A* **1999**, *103*, 11340.
(33) Cooper, W. F.; Park, J.; Hershberger, J. F. *J. Phys. Chem.* **1993**, *97*, 3283.
(34) Quandt, R. W.; Hershberger, J. F. *J. Phys. Chem.* **1996**, *100*, 9407.
(35) Rim, K. T.; Hershberger, J. F. *J. Phys. Chem. A* **1999**, *103*, 3721.
(36) Rothman, L. S.; Gamache, R. R.; Tipping, R. H.; Rinsland, C. P.; Smith, M. A. H.; Benner, D. C.; Devi, V. M.; Flaud, J. M.; Camy-Peyret, C.; Perrin, A.; Goldman, A.; Massie, S. T.; Brown, L. R.; Toth, R. A. *J. Quantum Spectrosc. Radiat. Transfer* **1992**, *48*, 469.
(37) Janz, G. J. *Inorganic Syntheses*; Mcgraw-Hill Book Company, Inc.: New York 1957; Vol. V.
(38) McKay, A. F. *J. Am. Chem. Soc.* **1948**, *70*, 1974.
(39) Stephenson, J. C.; Moore, C. B. *J. Chem. Phys.* **1970**, *52*, 2333.
(40) Fakhr, A.; Bates, R. D., Jr. *Chem. Phys. Lett.* **1980**, *71*, 381.
(41) Richman, D. C.; Millikan, R. C. *J. Chem. Phys* **1975**, *63*, 2242.
(42) Baren, R. E.; Erickson, M. A.; Hershberger, J. F. *Int. J. Chem. Kinet.* **2002**, *34*, 12.
(43) Rim, K. T.; Hershberger, J. F. *J. Phys. Chem. A* **2000**, *104*, 293.
(44) Glarborg, P.; Alzueta, M. U.; Dam-Johansen, K.; Miller, J. A. *Combust. Flame* **1998**, *115*, 1.
(45) Wang, N. S.; Yang, D. L.; Lin, M. C.; Melius, C. F. *Int. J. Chem. Kinet.* **1991**, *23*, 151.